# Unified Symmetry Classification of Magnetic Orders via Spin Space Groups: Prediction of Coplanar Even-Wave Phases

Ziyin Song,[1,2] Ziyue Qi,[1,2] Chen Fang,[1] Zhong Fang,[1,2] and Hongming Weng[1,3,*]

[1]*Beijing National Laboratory for Condensed Matter Physics, and Institute of Physics, Chinese Academy of Sciences, Beijing 100190, China*

[2]*University of Chinese Academy of Sciences, Beijing 100049, China*

[3]*Condensed Matter Physics Data Center, Chinese Academy of Sciences, Beijing 100190, China*

(Received 3 February 2026; revised 13 May 2026; accepted 14 July 2026; published 13 August 2026)

Spin space groups (SSGs) impose fundamentally different constraints on magnetic configurations in real and reciprocal spaces. As a consequence, the correspondence between real-space and momentum-space spin arrangements is far richer than traditionally assumed. Building on the complete enumeration of SSGs, we develop a systematic, symmetry-based framework that classifies all possible spin arrangements allowed by these groups. This unified approach naturally incorporates conventional magnetic orders, altermagnetism, and coplanar odd-wave magnetism (including the previously proposed $p$-wave case) as distinct symmetry classes. Moreover, by determining the symmetry-allowed wave patterns of spin-polarized phases, our framework classifies coplanar odd-wave magnets beyond the $p$-wave case into higher-wave types ($f$, $h$, $j$, and $l$ wave). Crucially, our classification predicts a variety of novel magnetic phases, highlighted by the discovery of the coplanar even-wave magnet(including $d$, $g$, and $i$ wave): A state that is noncollinear in real space but hosts a collinear even-wave spin polarization in $\mathbf{k}$ space. Analysis of a minimal model reveals that this phase is characterized by nonquantized spin polarization and exhibits a novel mechanism for symmetry-enforced zero polarization on nondegenerate bands. Extending the framework from bulk crystals to layer SSGs appropriate for two-dimensional systems, we further predict layered counterparts and provide symmetry guidelines for designing bilayer coplanar odd-wave and even-wave magnets. We further validate this finding through first-principles calculations and propose $CoCrO_4$ as a promising candidate for its experimental realization, thereby demonstrating the completeness and predictive power of the SSG-based classification of magnetic orders.

DOI: 10.1103/zy7s-j86r Subject Areas: Condensed Matter Physics, Magnetism

## I. INTRODUCTION

Symmetry lies at the heart of condensed matter physics. For magnetic materials, the presence of ordered moments breaks time-reversal symmetry, and their crystal symmetry is commonly described by magnetic space groups (MSGs) [1–3]. However, in the weak spin-orbit coupling (SOC) regime relevant for many magnets, the spin and lattice degrees of freedom decouple to a good approximation, since the crystal-field splitting, electron-electron interactions, and kinetic hopping amplitudes are all typically much larger than SOC. In this limit, it is natural to regard spin rotations as independent of spatial operations, which gives rise to the more general framework of spin space groups (SSGs) [4–6]. Many magnetic and transport properties are therefore governed primarily by SSG symmetries, with SOC acting merely as a perturbation [7,8]. Beyond these aspects, SSGs also refine the symmetry classification of band topology, enabling symmetry-enforced topological phases that are not captured by the conventional MSG description [6,9–15].

This SSG framework has recently attracted significant interest due to the discovery of altermagnetism [16–24], $p$-wave magnetism [25–29], and other unconventional magnetic phases [13,30–36]. Together with conventional ferromagnetism (FM) and antiferromagnetism (AFM), these phases exhibit distinct spin arrangements in real and reciprocal spaces, denoted by $S(\mathbf{r})$ and $S(\mathbf{k})$, respectively. Remarkably, altermagnets display zero net magnetization but exhibit spin splitting in reciprocal space, whereas $p$-wave magnetism, which is in fact one type of coplanar odd-wave magnetism [34], features coplanar spin arrangements in real space and collinear arrangements in reciprocal

[*]Contact author: hmweng@iphy.ac.cn

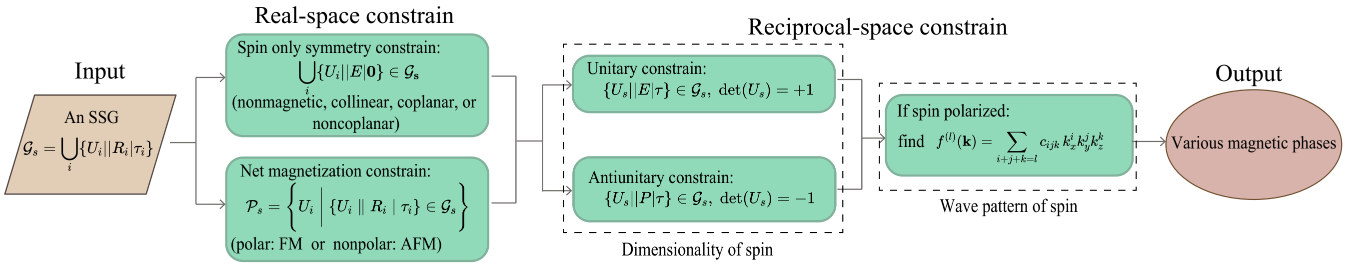


FIG. 1. Flowchart for the SSG-based classification of magnetic orders. Starting from an SSG $\mathcal{G}_s$, real-space constraints (left) determine the local spin configuration and whether a net magnetization is allowed. Reciprocal-space constraints (middle) fix the allowed spin textures $S(\mathbf{k})$, including their dimensionality and, for spin-polarized cases (dimension = 1), the corresponding wave pattern. The magnetic phases are obtained by combining the real- and reciprocal-space constraints (right).

space. Despite their apparent differences, these magnetic phases share a common origin: Their structures are fully dictated by how SSG operations constrain the spin configurations $S(\mathbf{r})$ and $S(\mathbf{k})$.

An SSG operation is written as $\{U_s||U_r|\tau\}$, where $U_s \in O(3)$ acts in spin space, $U_r$ is a spatial rotation, and $\tau$ is a translation. If $\det(U_s) = +1$, $U_s$ is a proper (unitary) spin rotation. If $\det(U_s) = -1$, the operation is antiunitary and includes time-reversal symmetry $\mathcal{T}$. In other words, any $U_s$ with $\det(U_s) = -1$ should be understood as $U_s = \tilde{U}_s\mathcal{T}$, where $\tilde{U}_s = \det(U_s)U_s$ is a proper spin rotation. Let $g_r = \{U_r|\tau\}$ and the action of $\{U_s||U_r|\tau\}$ on the spin configuration in real and reciprocal spaces reads

$$\{U_s||U_r|\tau\}S(\mathbf{r}) = U_s S(g_r^{-1}\mathbf{r}), \tag{1}$$

$$\{U_s||U_r|\tau\}S(\mathbf{k}) = U_s S[\det(U_s)g_r^{-1}\mathbf{k}], \tag{2}$$

where the key distinction is the appearance of the factor $\det(U_s)$ in reciprocal space. This additional sign causes certain symmetry operations to act differently on $S(\mathbf{r})$ and $S(\mathbf{k})$, thereby allowing distinct combinations of real-space and momentum-space spin textures. Altermagnetism and $p$-wave magnetism arise precisely from this fundamental difference.

Recently, all SSGs have been enumerated [37–39], providing a complete catalog of possible symmetry groups. However, the implications of these groups for constraining spin configurations—particularly for relating $S(\mathbf{r})$ and $S(\mathbf{k})$ within a unified framework—remain underdeveloped.

In this work, we present a comprehensive analysis of how SSG symmetries constrain spin arrangements in real and reciprocal spaces. Within this symmetry-based framework, we show that the recently proposed altermagnetic and $p$-wave magnetic phases naturally emerge as distinct SSG symmetry classes. Moreover, we demonstrate that additional unconventional magnetic textures, including coplanar even-wave phase, are also predicted within this framework.

This paper is organized as follows. In Sec. II, we analyze the SSG constraints on $S(\mathbf{r})$ and $S(\mathbf{k})$ for both three-dimensional bulk crystals and layered (two-dimensional) systems, and develop a general symmetry-based classification in Sec. III. Section IV introduces a minimal model for the coplanar $d$-wave magnetic phase and compares it with existing magnetic classes. In Sec. V, we propose a candidate material realization for this new phase. Finally, Sec. VII presents the discussion and concluding remarks.

## II. SYMMETRY CONSTRAINTS ON SPIN ARRANGEMENTS FROM SPIN SPACE GROUPS

In this section, we analyze how SSGs impose constraints on magnetic configurations in both real and reciprocal space. We show how these distinct constraints form the basis of a systematic classification of magnetic orders, as summarized in the flowchart in Fig. 1.

### A. Real-space constraints

We first examine the constraints imposed by SSGs on real-space magnetic configurations. These constraints fall into two distinct categories.

#### *1. Local on-site constraints*

If an on-site symmetry leaves an atomic position $\mathbf{r}$ invariant ($g_r^{-1}\mathbf{r} = \mathbf{r}$), it imposes a local condition on the magnetic moment,

$$S(\mathbf{r}) = U_s S(\mathbf{r}), \tag{3}$$

as expressed in Eq. (1). At a general Wyckoff position, only spin-only operations appear in the site symmetry. These can restrict the spins to be collinear or coplanar, whereas the presence of pure time-reversal symmetry forces $S(\mathbf{r}) = 0$, yielding a nonmagnetic configuration.

#### *2. Global constraints from the point group of the spin part*

The set of all spin rotations $\{U_s\}$ appearing in the SSG forms a point group in spin space (hereafter referred to as the point group of the spin part $\mathcal{P}_s$ to avoid confusion with the spin point group). Whether this group admits a nonzero invariant vector determines whether a uniform magnetization is symmetry allowed: Polar groups permit a net magnetic moment, whereas nonpolar groups forbid it. This provides the most general formulation of the FM-AFM dichotomy [8]: Polar $\mathcal{P}_s$ correspond to ferromagnetic-type orders, whereas nonpolar $\mathcal{P}_s$ correspond to antiferromagnetic-type orders.

Combining these on-site and spin-part constraints yields a systematic classification of real-space spin arrangements, including nonmagnetic, collinear, coplanar, and noncoplanar configurations, with an additional distinction based on whether a net magnetization is allowed (FM or AFM). In this paper, we pay more attention to the coplanar AFM types.

### B. Reciprocal-space constraints

We now turn to reciprocal space, where the constraints imposed by SSGs are typically richer and often more decisive for identifying the magnetic phase. We distinguish two aspects: (i) the dimensionality of the allowed spin texture and (ii) the symmetry-determined wave pattern of the spin polarization.

#### *1. Dimensionality of the spin texture*

At a generic momentum $\mathbf{k}$, the spin texture $S(\mathbf{k})$ is constrained by the little group at $\mathbf{k}$. The relevant on-site symmetries can be unitary or antiunitary. Unitary on-site operations take the form $\{U_s||E|\tau\}$ with $\det(U_s)=+1$. Antiunitary on-site symmetries may appear as $\{U_s||P|\tau\}$ with $\det(U_s)=-1$, where the $\mathbf{k}$ inversion induced by time reversal is compensated by spatial inversion $P$, making the operation on site at $\mathbf{k}$.

Because these operations act locally in $\mathbf{k}$ space, $S(\mathbf{k})$ must be invariant under the spin parts of all on-site symmetries:

$$\begin{aligned} &S(\mathbf{k}) = U_s S(\mathbf{k}),\\ \{U_s||E|\tau\}\in \mathrm{SSG},\qquad &\det(U_s)=+1,\\ \{U_s||P|\tau\}\in \mathrm{SSG},\qquad &\det(U_s)=-1. \end{aligned} \tag{4}$$

#### *2. Wave-pattern determination*

SSGs can also fix the wave pattern that characterizes the symmetry of the spin polarization in reciprocal space. We focus on symmetry-enforced spin-polarized phases, where at a generic $\mathbf{k}$ point the spin is constrained to lie along a fixed axis (e.g., the $z$ axis). In this case the polarization reduces to a scalar function $s(\mathbf{k})$. An SSG operation $\{U_s||U_r|\tau\}$ acts on $s(\mathbf{k})$ as

$$s(\mathbf{k}) = \begin{cases} +s(U_r^T\mathbf{k}) & \text{spin-preserving } U_s\\ -s(U_r^T\mathbf{k}) & \text{spin-flipping } U_s. \end{cases} \tag{5}$$

Thus, $s(\mathbf{k})$ carries a one-dimensional representation of the SSG, with character $+1$ for spin-preserving operations and $-1$ for spin-flipping operations.

We then define the wave number $l$ as the minimal total degree of a polynomial in $(k_x,k_y,k_z)$ that transforms according to this one-dimensional representation. Specifically, we consider

$$f^{(l)}(\mathbf{k}) = \sum_{i+j+k=l} c_{ijk}k_x^i k_y^j k_z^k, \tag{6}$$

with $i,j,k\in\mathbb{Z}_{\geq 0}$ and total degree $i+j+k=l$. For a given SSG, we determine the smallest integer $l>0$ for which there exists a nontrivial coefficient set $\{c_{ijk}\}$ such that

$$f^{(l)}(\mathbf{k}) = \begin{cases} +f^{(l)}(U_r^T\mathbf{k}) & \text{spin-preserving operations}\\ -f^{(l)}(U_r^T\mathbf{k}) & \text{spin-flipping operations.} \end{cases} \tag{7}$$

This is the same transformation law as for $s(\mathbf{k})$ above.

In group-theoretical language, the question is whether the SSG representation on the space of degree-$l$ polynomials contains a one-dimensional subrepresentation with the prescribed characters $\pm 1$. In practice, this amounts to solving a linear system for $\{c_{ijk}\}$ and is straightforward to implement numerically. The resulting $l$ agrees with the "characteristic spin-group integer" defined in terms of spin-degenerate nodal surfaces crossing the $\Gamma$ point in Ref. [16].

### C. Extension to layer condition

The discussion above applies to bulk (three-dimensional) crystals. For layered systems—i.e., systems with an open boundary condition along one direction (taken to be the $z$ axis without loss of generality)—the same unified symmetry constraints can be formulated using layer SSGs. In this case, the relevant spatial symmetry reduces from the 230 three-dimensional space groups to the 80 layer groups, and the corresponding SSG is built from these 80 layer groups [40].

For layer SSGs, the real-space constraints remain unchanged: Magnetic orders can still be classified as nonmagnetic, collinear, coplanar, or noncoplanar, with or without a net magnetization. In reciprocal space, however, the constraints at a generic in-plane momentum $\mathbf{k}=(k_x,k_y)$ become richer. In particular, we have

$$\begin{aligned} &S(\mathbf{k}) = U_s S(\mathbf{k}),\\ \{U_s||E|\tau\}\in \mathrm{SSG},\qquad &\det(U_s)=+1,\\ \{U_s||M_z|\tau\}\in \mathrm{SSG},\qquad &\det(U_s)=+1,\\ \{U_s||C_{2z}|\tau\}\in \mathrm{SSG},\qquad &\det(U_s)=-1,\\ \{U_s||P|\tau\}\in \mathrm{SSG},\qquad &\det(U_s)=-1. \end{aligned} \tag{8}$$

Within this framework, the dimensionality of the spin texture is classified in exactly the same way as for three-dimensional SSGs. Layer SSGs again allow 0D, 1D, 2D, and 3D spin textures in $\mathbf{k}$ space.

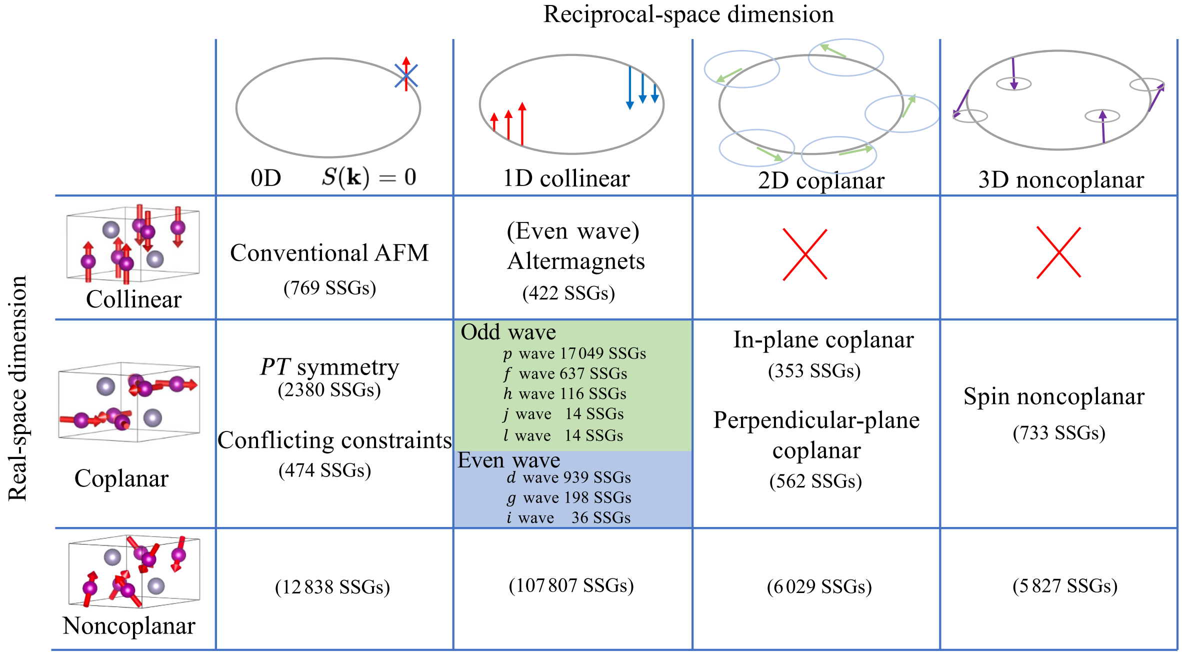


FIG. 2. Schematic SSG-based classification of magnetic orders with zero net magnetization. The table summarizes our classification of magnetic orders with zero net magnetization by combining the real-space spin geometry (rows: collinear, coplanar, and noncoplanar) with the allowed dimensionality of the generic-$\mathbf{k}$ spin texture $S(\mathbf{k})$ (columns: 0D, 1D, 2D, and 3D in reciprocal space). Each cell lists the corresponding symmetry class and the number of SSGs obtained from the complete enumeration. For collinear orders, the 0D and 1D columns reproduce conventional antiferromagnets and (even-wave) altermagnets, respectively. For coplanar orders, the 0D column includes $PT$-enforced nonmagnetic textures and textures suppressed by conflicting on-site constraints, while the 1D column splits into odd-wave and even-wave subclasses. The green and blue boxes highlight the symmetry-enforced coplanar spin-polarized classes discussed in this work: odd-wave (green) and coplanar even-wave (blue), together with wave-pattern subfamilies. The remaining cells indicate additional 2D or 3D spin textures allowed by SSG constraints, including spin-noncoplanar cases.

## III. CLASSIFICATION OF MAGNETIC ORDERS

By combining the reciprocal-space constraints with those in real space, we obtain a complete and systematic classification of magnetic orders. Building on the full enumeration of SSGs, this group-theoretical framework naturally reproduces all known collinear magnetic phases—including conventional antiferromagnetism and altermagnetism—while also revealing a broader landscape of coplanar orders.

In particular, for coplanar SSGs the reciprocal-space constraints allow a rich variety of spin textures, including odd-wave magnetism [34] and other nontrivial phases to be discussed below. The classification results for zero-magnetization magnetic orders are summarized in Fig. 2.

### A. Collinear configurations

A collinear SSG (1421 in total) is defined by a spin-only subgroup that preserves a single axis (without loss of generality, we choose the $z$ axis). This subgroup contains a unitary rotation $C_{nz}$ and an antiunitary mirror $M_x$. The operation $C_{nz}$ protects the collinear configuration in both real and reciprocal spaces, while the antiunitary $M_x$ imposes an even-wave constraint on the spin texture:

$$S^z(\mathbf{k}) = S^z(-\mathbf{k}), \tag{9}$$

ensuring that the spin polarization is symmetric under $\mathbf{k} \to -\mathbf{k}$.

The classification of collinear SSGs is determined by their point group of the spin part $\mathcal{P}_s$ together with the symmetry constraints at a generic $\mathbf{k}$ point in reciprocal space.

(1) $\mathcal{P}_s = 1$: No SSG operation reverses the spin direction. The absence of spin-flipping symmetries permits a net magnetization, resulting in a collinear ferromagnet with an even-wave spin-polarized Fermi surface. This class contains 230 SSGs, identical to the number of space groups.

(2) $\mathcal{P}_s = m$ (generated by $M_z$): The presence of $M_z$ (a spin-flip operation, equivalent to $C_{2x}$ or $C_{2y}$ in the presence of spin-only mirrors $M_x$ or $M_y$) forbids a net magnetization, leading to collinear antiferromagnetism. This AFM class further divides according to $\mathbf{k}$-space degeneracy.

(a) Conventional AFMs: These SSGs contain a degeneracy-enforcing constraint such as $\{M_z||P|\tau\}$ (an antiunitary operation involving inversion $P$) or $\{C_{2x(y)}||E|\tau\}$. These symmetries guarantee spin degeneracy at every $\mathbf{k}$ point, enforcing a vanishing reciprocal-space spin texture, $S(\mathbf{k}) = 0$. This class contains 769 SSGs. We note that although unitary and antiunitary degeneracy-enforcing mechanisms differ in other physical consequences (e.g., Berry curvature [11]), we do not distinguish them here since our focus is solely on the vanishing spin texture.

(b) Altermagnets: These SSGs also satisfy $\mathcal{P}_s = m$ (and therefore have zero net magnetization), but they lack the symmetries $\{M_z||P|\tau\}$ or $\{C_{2x(y)}||E|\tau\}$ that enforce band degeneracy. As a result, the band structure can be spin split, with a nonzero spin polarization $S(\mathbf{k})$ that alternates across the Brillouin zone and realizes characteristic even-wave patterns. This class contains 422 SSGs; the wave-pattern analysis yields 262 $d$-wave, 118$g$-wave, and 42$i$-wave cases.

Thus, this SSG-based classification naturally divides collinear orders into FM and AFM categories, with the AFM category further subdivided into conventional AFMs and altermagnets according to their $\mathbf{k}$-space symmetry. This classification of collinear SSGs has been established in previous works [37–39], and here we demonstrate how it follows directly from our general SSG-based framework.

## B. Coplanar configurations

Coplanar SSGs (24788 in total within 12× supercell [38]) are characterized by a spin-only antiunitary symmetry $M_z$ which confines spins to the $xy$ plane. This $M_z$ symmetry has two key consequences. First, it dictates the wave parity of the $\mathbf{k}$-space spin texture:

$$S(\mathbf{k}) = M_z S(-\mathbf{k}). \tag{10}$$

Since $M_z$ flips $S_z$ ($M_z S_z = -S_z$) but preserves $S_{x,y}$ ($M_z S_{x,y} = S_{x,y}$), this implies $S_z(\mathbf{k}) = -S_z(-\mathbf{k})$ (odd wave) while $S_{x,y}(\mathbf{k}) = S_{x,y}(-\mathbf{k})$ (even wave). Second, for every unitary operation $\{U_s||U_r|\tau\}$, a corresponding antiunitary counterpart $\{M_z U_s||U_r|\tau\}$ exists, enriching the $\mathbf{k}$-space constraints.

The point group of the spin part $\mathcal{P}_s$ for coplanar SSGs can be $C_{nz}$, $m$, or $C_{nv}$. The resulting $\mathbf{k}$-space spin textures are classified by their effective dimensionality (0D, 1D, 2D, or 3D) based on the on-site symmetry, such as $\{C_{nz}||E|\tau\}$, $\{C_{2x(y)}||E|\tau\}$, $\{M_z||P|\tau\}$, and $\{M_{x(y)}||P|\tau\}$.

### 1. Nonmagnetic (0D)

A nonmagnetic (0D) spin texture $[S(\mathbf{k}) = 0]$ implies a fully spin-degenerate band structure. This is enforced by two mechanisms:

(1) $PT$-like symmetry: The presence of a $PT$-like symmetry, such as $\{C_{2z}||P|\tau\}$ (noting $C_{2z}M_z = -1$), enforces spin degeneracy at every $\mathbf{k}$ point (2380 such SSGs).

(2) Conflicting constraints: A nonmagnetic state can also arise from mutually contradictory constraints. For example, two orthogonal on-site $C_2$ rotation symmetry operations, $\{C_2||E|\tau_1\}$ and $\{C_2'||E|\tau_2\}$, may enforce $S(\mathbf{k})$ to lie along two different, perpendicular axes, for which the only solution is $S(\mathbf{k}) = 0$ (474 SSGs).

### 2. Spin polarized (1D)

A 1D (spin-polarized) $\mathbf{k}$-space texture occurs when SSG stabilizers constrain $S(\mathbf{k})$ to a single, fixed axis. This class reveals two physically distinct patterns:

(1) $z$-axis polarization (odd wave): The stabilizer $\{C_{nz}||E|\tau\}$ $(n \geq 2)$ constrains $S(\mathbf{k})$ to lie along the $z$ axis. Together with Eq. (10), this enforces an odd-wave $z$-polarized texture:

$$S^z(\mathbf{k}) = -S^z(-\mathbf{k}). \tag{11}$$

Such symmetry-enforced coplanar odd-wave patterns were also discussed in Ref. [34]; in our enumeration they are realized by 17830 distinct coplanar SSGs. These SSGs can be further classified by the symmetry of their reciprocal-space spin polarization into $p$-wave [25] (17049 SSGs), $f$-wave [34] (637), $h$-wave (116), $j$-wave (14), and $l$-wave (14) subclasses.

While the stabilizer $\{C_{nz}||E|\tau\}$ $(n \geq 2)$ can in principle take arbitrarily large values—allowing incommensurate or spiral structures—the chosen cutoff of 12× supercell is sufficiently large and highly factorable to include all physically relevant commensurate phases. In practice, all commensurate odd-wave phases identified in the MAGNDATA database satisfy this cutoff.

(2) In-plane polarization (even wave): The stabilizer $\{C_{2x(y)}||E|\tau\}$ constrains $S(\mathbf{k})$ to lie along the $x$ ($y$) axis, i.e., within the coplanar plane. Equation (10) then requires the in-plane polarization to be even wave:

$$S^{x(y)}(\mathbf{k}) = S^{x(y)}(-\mathbf{k}). \tag{12}$$

This symmetry-enforced even-wave spin polarization defines a distinct phase predicted by our classification. Our SSG enumeration shows that this class contains 517 polar SSGs (FM type). This number coincides with that of type-IV MSGs, because these SSGs can be generated by combining a (nonmagnetic) space group with the spin-translation operation $\{C_{2x(y)}||E|\tau\}$. In addition, the same construction yields 1173 nonpolar SSGs (AFM type), among which 939 realize $d$-wave, 198 realize

$g$-wave, and 36 realize $i$-wave even-spin textures. These numbers are exact within our classification scheme, where the SSG is restricted to a twofold supercell of the parent space group.

In Sec. IV and Supplemental Material [41], we discuss this coplanar even-wave phase (including the $\mathbf{k}$-space $d$-wave and higher-order moments) in detail, including minimal models for different wave numbers and its many-to-one mapping to the altermagnetic phase.

#### 3. Spin coplanar (2D)

A 2D (spin-coplanar) texture in $\mathbf{k}$ space is realized when $S(\mathbf{k})$ is constrained to a plane but not to a line. This arises from antiunitary mirrorlike symmetries of the form $\{M||P|\tau\}$. We identify two types:

(1) In-plane coplanar: The operation $\{M_z||P|\tau\}$ (actually a pure inversion symmetry combined with the spin-only $M_z$) enforces $S(\mathbf{k})$ to lie within the $xy$ plane for all $\mathbf{k}$. This results in a coplanar texture in both real and reciprocal space (605 SSGs: 252 polar, 353 nonpolar).

(2) Perpendicular-plane coplanar: The operation $\{M_{x(y)}||P|\tau\}$ enforces $S(\mathbf{k})$ to lie within a plane perpendicular to the real-space spin plane (e.g., the $xz$ or $yz$ plane). This is a nontrivial case where the real-space and $\mathbf{k}$-space coplanar planes are mutually orthogonal (814 SSGs: 252 polar, 562 nonpolar).

#### 4. Spin noncoplanar (3D)

Finally, if an SSG lacks any of the $\mathbf{k}$-space on-site symmetries that constrain the dimensionality (0D, 1D, or 2D), the spin arrangement in reciprocal space is unconstrained. At a generic $\mathbf{k}$ point, $S(\mathbf{k})$ is free to point in any direction, resulting in a generic noncoplanar (3D) spin texture. This constitutes the most general case (995 SSGs: 262 polar, 733 nonpolar).

### C. Noncoplanar configurations

Finally, we consider noncoplanar SSGs. These groups are defined by the absence of any nontrivial spin-only symmetry. Consequently, their real-space spin textures lack an intrinsic characteristic direction, such as the collinear axis or the coplanar plane found in the other classes.

Despite this lack of real-space constraint, the reciprocal-space spin texture $S(\mathbf{k})$ can still be highly constrained by $\mathbf{k}$-space stabilizers. Our SSG enumeration finds that these noncoplanar SSGs can produce a variety of $\mathbf{k}$-space spin arrangements, including the following:

(1) Nonmagnetic (0D): A total of 12838 SSGs enforce a nonmagnetic $S(\mathbf{k})=0$ texture. As in the coplanar case, this is typically protected by a $PT$-like symmetry or by contradictory on-site symmetry constraints.

(2) Spin polarized (1D): A total of 127146 SSGs enforce a collinear $\mathbf{k}$-space spin texture, protected by an on-site symmetry operation such as $\{C_n||E|\tau\}$.

(3) Spin coplanar (2D): A total of 8323 SSGs enforce a coplanar $S(\mathbf{k})$ texture, protected by an on-site symmetry such as $\{M||P|\tau\}$.

(4) Spin noncoplanar (3D): A total of 8982 SSGs, which lack any of the $\mathbf{k}$-space on-site symmetry constraints required for 0D, 1D, or 2D arrangements.

### D. Classification for layered magnetic orders

As we have shown, the symmetry constraints imposed by SSGs can be formulated straightforwardly for layered systems. The unified symmetry classification of magnetic orders developed above therefore applies equally well to layered magnetic orders.

For collinear orders, this construction reproduces the family of layered altermagnets, which break spin-flip symmetry through the layer operations $\{M_z|\tau\}$, $\{P|\tau\}$, $\{E|\tau\}$, and $\{C_{2z}|\tau\}$. These four operations are precisely the layer counterparts generated by the replacements discussed above, and this family has been analyzed previously in Refs. [49–51].

This layer-based symmetry classification is particularly convenient for designing coplanar odd-wave (including $p$-wave) magnets [34] and coplanar even-wave magnets in bilayer structures. In strictly three-dimensional crystals, a collinear reciprocal-space spin texture can only be protected by a symmetry of the form $\{C_2||E|\tau\}$, i.e., a spin rotation combined with a pure translation, which can be uncommon in realistic materials. In contrast, in layered systems one may construct a bilayer from two coplanar layers related by a symmetry of the form $\{C_2||M_z\}$, where the $C_2$ axis is either perpendicular or parallel to the coplanar plane. The former realizes a coplanar odd-wave magnetic phase, whereas the latter realizes a coplanar even-wave magnetic phase.

This design principle is implemented explicitly in Supplemental Material [41], where we construct concrete bilayer models for coplanar even-wave phases. Furthermore, we propose a strategy to realize a coplanar even-wave phase by stacking two monolayer altermagnets, which allows continuous tuning of the spin polarization within this phase.

## IV. MODEL OF COPLANAR $d$-WAVE MAGNETISM

In this section, we present a minimal model for a coplanar $d$-wave magnetic phase. We highlight its critical differences from coplanar odd-wave magnetism, which can share a similar real-space spin configuration, and from $d$-wave altermagnetism, which exhibits a similar $\mathbf{k}$-space symmetry. The construction of minimal models for other coplanar even-wave magnetic phases is presented in Supplemental Material [41].

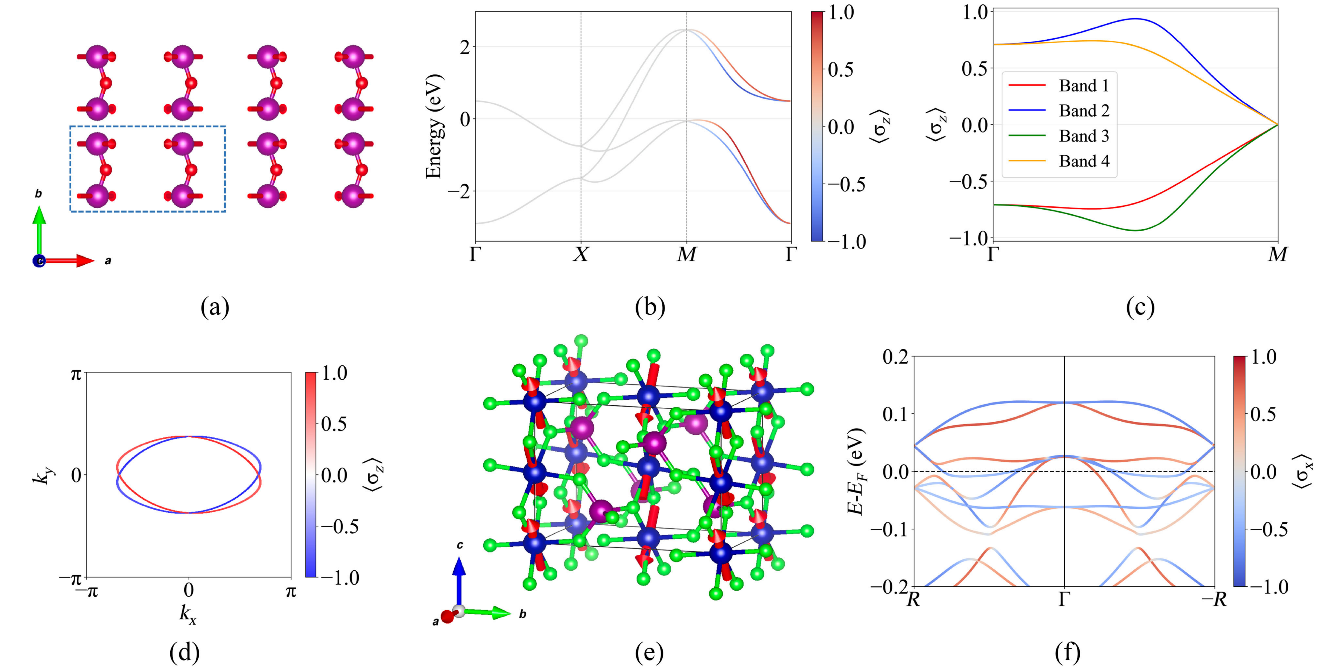


FIG. 3. (a) Real-space lattice model for the coplanar $d$-wave magnet, fulfilling the required SSG symmetries. The dashed box indicates the magnetic unit cell. (b) Calculated band structure along high-symmetry lines and spin polarization ($\langle S_z \rangle$) projected onto the bands. (c) Spin polarization ($\langle S_z \rangle$) of four bands along the $\Gamma - M$ path. (d) Spin-polarized Fermi surface at $\mu = -2$ eV, showing the characteristic $d$-wave anisotropy. (e) Magnetic structure of $CoCrO_4$ exhibiting the coplanar magnetic configuration. (f) First-principles band structure of $CoCrO_4$ and spin polarization ($\langle S_x \rangle$) projected onto the bands along the high-symmetry path.

### A. Symmetry and model Hamiltonian

We consider a model based on the real-space configuration shown in Fig. 3(a), which features four magnetic atoms per unit cell. The magnetic moments are $(\alpha, 0, \beta)$, $(-\alpha, 0, \beta)$, $(\alpha, 0, -\beta)$, and $(-\alpha, 0, -\beta)$, respectively. This arrangement yields zero net magnetization and a spin configuration that is coplanar in the $xz$ plane, consistent with the spin-only antiunitary symmetry $\{M_y || E\}$.

Despite the real-space coplanarity, the reciprocal-space spin texture is constrained by the SSG to be collinear and $z$ polarized. The symmetry constraints in the reciprocal space are

$$\begin{aligned} \{C_{2z} || t\}&:\ S_x(k_x, k_y) = 0;\ S_y(k_x, k_y) = 0, \\ \{M_y || E\}&:\ S_z(k_x, k_y) = S_z(-k_x, -k_y), \\ \{C_{2x} || M_y\}&:\ S_z(k_x, k_y) = -S_z(k_x, -k_y). \end{aligned} \tag{13}$$

The first constraint, $\{C_{2z} || t\}$, enforces a pure $z$-axis spin polarization in $\mathbf{k}$ space. The second, $\{M_y || E\}$, dictates an even-wave parity under inversion. The third, $\{C_{2x} || M_y\}$, enforces an odd parity under reflection $k_y \to -k_y$. This momentum-space symmetry is precisely that of a $d$-wave state.

We then construct a minimal effective Hamiltonian for the nonmagnetic sites that respects these symmetries, and the detailed derivation is given in Supplemental Material [41]:

$$\begin{aligned} \mathcal{H}(\mathbf{k}) = {} & 2t_0 \cos\frac{k_x}{2} \sigma_0 \tau_1 + 2t_0 \cos k_y \sigma_0 \tau_0 \\ & + [t_1 \cos k_x + t_2 \cos k_y] \sigma_1 \tau_3 \\ & + t_3 \sin\frac{k_x}{2} \sigma_1 \tau_2 + t_4 \sin k_y \sigma_2 \tau_3, \end{aligned} \tag{14}$$

where $\sigma_i$ and $\tau_i$ are Pauli matrices for the spin and sublattice degrees of freedom, respectively. The calculations are performed using the hopping parameters $t_0 = -0.6$, $t_1 = 0.5$, $t_2 = 0.7$, $t_3 = 0.4$, and $t_4 = 0.6$.

The resulting band structure and spin polarization projected onto the bands are presented in Fig. 3. Figure 3(b) shows the band structure along high-symmetry paths. Along the $\Gamma - X$ path, the bands are doubly degenerate and the total spin polarization $S_z(\mathbf{k})$ is zero, as the degeneracy is protected by the $\{C_{2x} || M_y\}$ symmetry. The $X - M$ path is nondegenerate, yet the expectation value of the spin polarization is still enforced to be zero by the $\{M_z || M_y\}$ symmetry. The $M - \Gamma$ path is nondegenerate and exhibits a finite spin polarization along the $z$ axis.

Figure 3(c) plots the expectation value of spin polarization $\langle S_z \rangle$ for these four bands along the $\Gamma - M$ path, where the expectation values of $\langle S_x \rangle$ and $\langle S_y \rangle$ are zero and therefore not shown. Finally, Fig. 3(d) displays the spin-polarized Fermi surface at $\mu = -2$ eV, which shows

TABLE I. Comparison of the symmetry properties of collinear altermagnets, coplanar odd-wave magnets, and coplanar even-wave magnetic orders. For clarity, we adopt a coordinate convention in which the spin polarization in momentum space is chosen along the $z$ axis for all three phases: The real-space moments are then collinear along $z$ for the altermagnet, coplanar in the $xy$ plane for the coplanar odd-wave phase, and coplanar in a plane containing the $z$ axis (e.g., $xz$ or $yz$) for the coplanar even-wave phase.

| | Collinear altermagnet | Coplanar odd wave | Coplanar even wave |
|---|---|---|---|
| Spin polarization (**k** space) | $\{C_{\infty z}\|\|E\}$ | $\{C_{nz}\|\|E\|\tau\}$ | $\{C_{2z}\|\|E\|\tau\}$ |
| Collinear (**r** space) | $\{C_{\infty z}\|\|E\}$ | × | × |
| Coplanar (**r** space) | × | $\{M_z\|\|E\}$ | $\{M_{x/y}\|\|E\}$ |
| $\varepsilon_\uparrow(\mathbf{k}) = \varepsilon_\downarrow(-\mathbf{k})$ | × | $\{M_z\|\|E\}$ | × |
| $\varepsilon_\uparrow(\mathbf{k}) = \varepsilon_\uparrow(-\mathbf{k})$ | $\{M_{x,y}\|\|E\}$ | × | $\{M_{x/y}\|\|E\}$ |
| Spin polarization direction | $S(\mathbf{k})\|\|S(\mathbf{r})$ ($z$ axis) | $S(\mathbf{k}) \perp S(\mathbf{r})$ plane | $S(\mathbf{k})\|\|S(\mathbf{r})$ plane ($yz$ or $xz$ plane) |
| Spin a good quantum number? | ✓ | × | × |

the characteristic $d$-wave anisotropy of this magnetic phase. Further analyses and model Hamiltonians for a coplanar $d$-wave phase with $C_4$ symmetry, as well as coplanar $g$- and $i$-wave phases, are presented in Supplemental Material [41].

### B. Distinction from other phases

In Table I, we compare the symmetry properties of collinear altermagnets, coplanar odd-wave, and coplanar even-wave magnetic orders. For coplanar odd-wave magnetism, the **k**-space spin polarization is perpendicular to the real-space spin plane, whereas for the coplanar even wave, it is parallel to the real-space spin plane. Consequently, their respective spin-only symmetries result in different **k**-space parities: Coplanar odd-wave magnetism exhibits an odd-wave pattern, while the coplanar even wave exhibits an even-wave pattern. Thus, the coplanar even wave is a new phase that simultaneously shows similarities with collinear altermagnetism (even-wave parity) and coplanar odd-wave magnetism (coplanar in real space, collinear in **k** space). We further show that coplanar even-wave SSGs admit a many-to-one mapping onto altermagnetic SSGs, as detailed in Supplemental Material [41].

It is crucial to emphasize another fundamental difference between this coplanar even-wave phase and collinear altermagnetism, even though both exhibit $z$-axis spin polarization and even-wave parity in **k** space. (This distinction also applies when comparing coplanar odd-wave magnetism with altermagnetism.)

In the collinear altermagnet, spin is a good quantum number. The Hamiltonian contains only $\sigma_0$ and $\sigma_3$ terms, and the eigenstates are pure spin-up or spin-down, i.e., $\langle\sigma_z\rangle = \pm 1$.

In our coplanar model (the same as in coplanar odd-wave magnetism), the Hamiltonian explicitly contains $\sigma_1$ and $\sigma_2$ terms. Consequently, spin is not a good quantum number, and the spin rotation symmetry $C_{nz}$ is broken. Although the spin expectation value $\vec{M} = (\langle\sigma_x\rangle, \langle\sigma_y\rangle, \langle\sigma_z\rangle)$ is polarized along $z$ (i.e., $M_x = M_y = 0$ and $M_z/|\vec{M}| = 1$ due to the $\{C_{2z}\|t\}$ symmetry), the local eigenstates are not pure spin states. As shown in Fig. 3(c), the spin polarization varies continuously along the $\Gamma - M$ path, approaching zero smoothly as it reaches the $M$ point.

Moreover, this coplanar model exhibits a crucial distinction from collinear altermagnetism in how its spin polarization vanishes. In collinear altermagnets, $S_z(\mathbf{k})$ vanishes only on high-symmetry paths where spin degeneracy is protected. Our model shows this conventional behavior along the $\Gamma - X$ path [Fig. 3(b)], where $S_z = 0$ because the degeneracy is protected by the symmetry $\{C_{2x}\|M_y\}$.

However, a novel mechanism is observed along the $X - M$ path. Here, the bands are clearly nondegenerate, yet the spin polarization $S_z(\mathbf{k})$ is still forced to be zero. This is a direct consequence of the on-site symmetry $\{M_z\|M_y\}$. As this symmetry is antiunitary and squares to $+1$ (not $-1$), it does not protect band degeneracy. Instead, it reverses the spin polarization operator ($S_z \to -S_z$), forcing its expectation value to vanish along the entire $X - M$ path. This explains why the spin polarization smoothly reaches zero precisely at the $M$ point, as observed in Fig. 3(c).

## V. MATERIAL REALIZATION: $CoCrO_4$

Our SSG-based framework provides a practical workflow for material classification: Starting from an experimentally determined magnetic structure, one can identify its SSG and assign it to one of the symmetry classes in our scheme. By analyzing the magnetic structures in the MAGNDATA database [52], we find 73 entries (including CeNiAsO proposed in Ref. [25]) whose SSGs and magnetic configurations realize coplanar odd-wave magnets, defined as states with coplanar local moments, zero net magnetization, and a collinear spin polarization in momentum space perpendicular to the spin plane. In this search we did not require all magnetic atoms to be related by SSG operations (i.e., magnetically inequivalent sites are allowed). The MAGNDATA identifiers and chemical formulas of these 73 candidates are listed in Supplemental Material [41].

In addition, we identify cobalt chromate $CoCrO_4$ as a promising candidate material for coplanar even-wave magnet. According to neutron diffraction studies, $CoCrO_4$ is isostructural with $CrVO_4$ and crystallizes in the orthorhombic space group *Cmcm* (no. 63). The magnetic $Co^{2+}$ ions are located at the Wyckoff positions (0, 0, 0), (0, 0, 1/2), (1/2, 1/2, 1/2), and (1/2, 1/2, 0) within the unit cell [52–54].

Crucially, the experimentally determined magnetic structure is noncollinear. As depicted in Fig. 3(e), the arrangement of the magnetic $Co^{2+}$ spins (represented by the red arrows on the blue Co atoms) is characterized by a combination of $A_x$ and $G_z$ modes. (The blue spheres represent Co atoms, the purple spheres represent Cr atoms, and the green spheres represent O atoms.) This superposition results in a coplanar spin texture where all magnetic moments lie in the $xz$ plane (at an angle of 55° with the $x$ axis). This real-space structure corresponds to a coplanar SSG whose spin-only point group is generated by $\{M_y||E\}$.

The full SSG is generated by operations including $\{E||P\}$, $\{C_{2y}||C_{2z}|0,0,\frac{1}{2}\}$, $\{E||C_{2x}\}$, and $\{C_{2x}||E|\frac{1}{2}\frac{1}{2}0\}$. This SSG falls into the coplanar $d$-wave class identified in Sec. II. Specifically, the operation $\{C_{2x}||E|\frac{1}{2}\frac{1}{2}0\}$ constrains the reciprocal-space spin arrangement to be polarized along the $x$ axis $[S_y(\mathbf{k}) = S_z(\mathbf{k}) = 0]$.

It is crucial to justify the use of the SSG framework here. First, this SSG is fully compatible with the nonmagnetic space group (*Cmcm*), as every spatial operation in *Cmcm* is paired with a specific spin operation to form an element of the SSG. Second, The magnetic space group for this structure is *Pbcn*, with the Belov-Neronova-Smirnova (BNS) notation No. 60.417, which contains only one-fourth of the symmetry operations present in the full SSG. The MSG framework is therefore insufficient, and the SSG provides a richer, more accurate description. Finally, this approach is physically appropriate, as $CoCrO_4$ is composed of $3d$ elements (Cr, Co) where SOC is weak, validating the decoupling of spin and spatial operations. The effects of SOC on the electronic structure and transport are analyzed in detail in Supplemental Material [41].

To confirm this prediction, we performed first-principles calculations and the computational details are given in Supplemental Material [41]. Figure 3(f) shows the calculated band structure and spin polarization of $CoCrO_4$ along the $R(0,\pi/2,\pi/2)$ to $\Gamma(0,0,0)$ to $-R[0,-(\pi/2),-(\pi/2)]$ path. The bands are clearly spin polarized. As required by the SSG symmetry, the spin polarization is purely along the $x$ axis (polarization components along other axes are zero and not shown). Furthermore, the plot demonstrates the even-wave symmetry of this polarization, as $S_x(\mathbf{k}) = S_x(-\mathbf{k})$ (i.e., the polarization is identical on the $\Gamma \to R$ and $\Gamma \to -R$ segments). This even parity is a direct consequence of the spin-only symmetry $\{M_y||E\}$, as discussed in Sec. II.

We also note that the spin polarization is separately forced to zero on the $k_y = 0$ and $k_z = 0$ planes. This is an additional constraint enforced by the little group symmetries $\{M_y||C_{2z}|0,0,\frac{1}{2}\}$ and $\{M_z||C_{2z}|0,0,\frac{1}{2}\}$, respectively.

## VI. SYMMETRY CONSTRAINTS ON TRANSPORT TENSORS

In this section, we briefly review the established symmetry framework for classifying response tensors based on spin groups, spin point groups, and generalized Jahn symbols, with particular emphasis on the distinction between SOC-free and SOC-induced responses. We then apply this framework to the coplanar even-wave magnetic phase introduced in this work and compare its symmetry-allowed response tensors with those of the corresponding altermagnet. We show that the two phases obey identical symmetry constraints for tensors without spin indices and for tensors with a single spin index, whereas distinct constraints can emerge for tensors involving multiple spin indices.

The symmetry classification of physical response tensors in magnetic systems has been systematically developed in previous works using magnetic groups, spin groups, spin point groups, and generalized Jahn symbols [55–60]. Within this established framework, SSG symmetries and Jahn symbols determine the symmetry-allowed tensor components, which can be divided into SOC-free and SOC-induced parts. The SOC-induced components are forbidden by SSG symmetry but allowed by MSG symmetry; a representative example is the anomalous Hall effect in altermagnets, where the anomalous Hall conductivity (AHC) is $T$ odd, but the spin-only symmetry of a collinear SSG forbids it. Therefore, the analysis of SOC-induced transport requires combining MSG and SSG constraints or using oriented spin-space groups [8]. In this work, we focus on transport tensors allowed without SOC.

We next apply this framework to the coplanar even-wave magnetic phase. The difference between altermagnetism and coplanar even-wave magnetism in this analysis arises from their distinct spin-only symmetries. Take $CoCrO_4$ as an example. Its spin point group contains the generators $\{C_{2x}||E\}$, $\{M_y||E\}$, $\{E||P\}$, $\{C_{2y}||C_{2z}\}$, and $\{E||C_{2x}\}$. Notably, the spin-translation operation $\{C_{2x}||E|\frac{1}{2}\frac{1}{2}0\}$ acts equivalently to a spin-only symmetry in constraining tensors. Replacing $\{C_{2x}||E\}$ with $\{C_{\infty x}||E\}$, which denotes arbitrary rotations about $x$, yields the corresponding altermagnet. For transport tensors without spin indices (e.g., AHC, Nernst), both groups impose the same constraints, equivalent to those of the gray group of the parent space group, because $\{M_y||E\}$ acts as a pure time-reversal operation.

For tensors with a single spin index (first-order spin transport, i.e., tensors containing only one $M$ in their Jahn symbol), altermagnets and coplanar even-wave magnets share the same symmetry constraints. A representative example of such a tensor is the $T$-odd spin conductivity [61–63] (Jahn symbol $MV2$).

Denoting a general tensor as $\chi^{k}_{i_1 i_2\ldots}$, where $k$ is the spin index and $i_1, i_2, \ldots$ are real-space indices, the generators $\{C_{2x}||E\}$ and $\{C_{\infty x}||E\}$ enforce that all components with spin along $y$ or $z$ vanish, so that only the spin-$x$ component is allowed. Similarly, for the spin conductivity of $CoCrO_4$, the $T$-even components are entirely forbidden by symmetry, while the $T$-odd components are restricted by $\{C_{2y}||C_{2z}\}$ and $\{E||C_{2x}\}$ such that only the $yz$ and $zy$ components of the spin-$x$ conductivity are nonzero. These surviving components are independent, consistent with the corresponding altermagnet.

For tensors with more than one spin index, the constraints differ. Consider a tensor $\chi^{k_1 k_2}$ (Jahn symbol $M2$). For a coplanar even-wave magnet, the SSG operations $\{M_y||E\}$ and $\{C_{2x}||E\}$ force all off-diagonal components to vanish, so that only the diagonal components survive and are independent. In contrast, for the corresponding altermagnet with $\{C_{\infty x}||E\}$, isotropy in the $yz$ plane imposes an additional constraint, leaving only two independent diagonal components:

$$\chi^{xx}, \qquad \chi^{yy} = \chi^{zz}. \tag{15}$$

This illustrates how coplanar even-wave and altermagnetic phases impose different symmetry constraints on higher-order spin transport tensors.

In Supplemental Material [41], we further analyze the symmetry of a constructed bilayer coplanar even-wave structure, calculate the corresponding response tensors, and compare them with those of the corresponding altermagnet.

## VII. CONCLUSIONS AND OUTLOOK

In this work, we have developed a comprehensive and systematic classification of magnetic orders based on SSG symmetries. Our framework is built upon the fundamental principle that SSGs impose distinct constraints on spin configurations in real space [$S(\mathbf{r})$] and reciprocal space [$S(\mathbf{k})$]. This discrepancy, which originates from the $\det(U_s)$ factor in the momentum-space transformation, allows for a rich variety of magnetic phases beyond conventional classifications.

Using the complete enumeration of SSGs, we have shown that our framework provides a unified understanding of known magnetic orders. It naturally incorporates conventional ferromagnetism and antiferromagnetism, as well as the recently discovered unconventional phases of altermagnetism and $p$-wave magnetism, as distinct symmetry classes.

More importantly, our systematic approach predicts a variety of novel magnetic states, including higher-wave coplanar odd-wave magnets and coplanar even-wave magnets. We have focused on the coplanar even-wave magnet, which features a coplanar real-space spin arrangement while hosting a collinear, even-wave spin polarization in reciprocal space. We presented a minimal model for this phase and highlighted its distinctive properties, including a nonquantized spin polarization and a mechanism for symmetry-enforced vanishing polarization [$S_z(\mathbf{k}) = 0$] on nondegenerate bands. Furthermore, we identified $CoCrO_4$, with its coplanar magnetic structure, as a promising candidate material for experimental realization.

Looking forward, the classification framework presented here provides a powerful road map for the discovery and identification of new unconventional magnetic materials. While we focused on the coplanar even-wave phase, our analysis revealed many other exotic possibilities, particularly within the coplanar and noncoplanar SSGs (e.g., states with $\mathbf{k}$-space coplanar spin configuration), which represent a new frontier for theoretical and experimental exploration.

Investigating the physical consequences of these new magnetic orders is a critical next step. For instance, the unique interplay of noncollinear real-space spins and collinear, even-wave momentum-space spins in the coplanar even-wave phase may lead to novel magnetotransport and optical responses, distinct from both altermagnets and $p$-wave magnets. Finally, we call for further experimental investigation of our candidate material, $CoCrO_4$, using techniques such as spin-polarized angle-resolved photoemission spectroscopy (ARPES), to directly visualize the predicted $d$-wave spin polarization in its Fermi surface and confirm its status as the first coplanar even-wave magnet.

## ACKNOWLEDGMENTS

This work was supported by the Science Center of the National Natural Science Foundation of China (Grants No. 12188101 and No. 12325404), the National Key R&D Program of China (Grants No. 2022YFA1403800, No. 2023YFA1607400, No. 2024YFA1408400 and No. 2023YFA1406704), the National Natural Science Foundation of China (Grants No. 12274436, No. 11921004, and No. 12547112), the Strategic Priority Research Program (B) of the Chinese Academy of Sciences (CAS) (Grant No. XDB1720000), and H. W. acknowledges support from the New Cornerstone Science Foundation through the XPLORER PRIZE.

## DATA AVAILABILITY

The data that support the findings of this article are available in Supplemental Material [41] and in the SSGClassify GitHub repository [64].

[1] C. J. Bradley and B. L. Davies, *Magnetic groups and their corepresentations*, Rev. Mod. Phys. **40**, 359 (1968).
[2] Ron Lifshitz, *Magnetic point groups and space groups*, in *Encyclopedia of Condensed Matter Physics (Second Edition)*, edited by Tapash Chakraborty (Academic Press, Oxford, 2024), pp. 1–10.

[3] Daniel B. Litvin, Magnetic Group Tables: 1-, 2- and 3-Dimensional Magnetic Subperiodic Groups and Magnetic Space Groups (International Union of Crystallography, Chester, 2013).
[4] D. B. Litvin and W. Opechowski, *Spin groups*, Physica **76**, 538 (1974).
[5] W. F. Brinkman and R. J. Elliott, *Theory of spin-space groups*, Proc. R. Soc. A **294**, 343 (1966).
[6] Pengfei Liu, Jiayu Li, Jingzhi Han, Xiangang Wan, and Qihang Liu, *Spin-group symmetry in magnetic materials with negligible spin-orbit coupling*, Phys. Rev. X **12**, 021016 (2022).
[7] Zheng Liu, Mengjie Wei, Wenzhi Peng, Dazhi Hou, Yang Gao, and Qian Niu, *Multipolar anisotropy in anomalous Hall effect from spin-group symmetry breaking*, Phys. Rev. X **15**, 031006 (2025).
[8] Yuntian Liu, Xiaobing Chen, Yutong Yu, Jesús Etxebarria, J. Manuel Perez-Mato, and Qihang Liu, *Symmetry classification of magnetic orders using oriented spin space groups*, Nature (London) **652**, 869 (2026).
[9] Jian Yang, Zheng-Xin Liu, and Chen Fang, *Symmetry invariants and classes of quasiparticles in magnetically ordered systems having weak spin-orbit coupling*, Nat. Commun. **15**, 10203 (2024).
[10] Peng-Jie Guo, Yi-Wen Wei, Kai Liu, Zheng-Xin Liu, and Zhong-Yi Lu, *Eightfold degenerate fermions in two dimensions*, Phys. Rev. Lett. **127**, 176401 (2021).
[11] Pengfei Liu, Ao Zhang, Jingzhi Han, and Qihang Liu, *Chiral Dirac-like fermion in spin-orbit-free antiferromagnetic semimetals*, Innovation **3**, 100343 (2022).
[12] A. Corticelli, R. Moessner, and P. A. McClarty, *Spin-space groups and magnon band topology*, Phys. Rev. B **105**, 064430 (2022).
[13] Xiaobing Chen, Yuntian Liu, Pengfei Liu, Yutong Yu, Jun Ren, Jiayu Li, Ao Zhang, and Qihang Liu, *Unconventional magnons in collinear magnets dictated by spin space groups*, Nature (London) **640**, 349 (2025).
[14] Sheng Zhang, Ziyin Song, Zhong Fang, Hongming Weng, and Zhijun Wang, *IRSSG: An open-source software package for spin space groups*, Comput. Phys. Commun. **326**, 110190 (2026).
[15] Ziyin Song, A. Z. Yang, Yi Jiang, Zhong Fang, Jian Yang, Chen Fang, Hongming Weng, and Zheng-Xin Liu, *Constructions and applications of irreducible representations of spin-space groups*, Phys. Rev. B **111**, 134407 (2025).
[16] Libor Šmejkal, Jairo Sinova, and Tomas Jungwirth, *Beyond conventional ferromagnetism and antiferromagnetism: A phase with nonrelativistic spin and crystal rotation symmetry*, Phys. Rev. X **12**, 031042 (2022).
[17] Libor Šmejkal, Jairo Sinova, and Tomas Jungwirth, *Emerging research landscape of altermagnetism*, Phys. Rev. X **12**, 040501 (2022).
[18] Igor Mazin (The PRX Editors), *Editorial: Altermagnetism—A new punch line of fundamental magnetism*, Phys. Rev. X **12**, 040002 (2022).
[19] Yusuke Noda, Kaoru Ohno, and Shinichiro Nakamura, *Momentum-dependent band spin splitting in semiconducting* $MnO_2$*: A density functional calculation*, Phys. Chem. Chem. Phys. **18**, 13294 (2016).
[20] Libor Šmejkal, Rafael González-Hernández, T. Jungwirth, and J. Sinova, *Crystal time-reversal symmetry breaking and spontaneous Hall effect in collinear antiferromagnets*, Sci. Adv. **6**, eaaz8809 (2020).
[21] Kyo-Hoon Ahn, Atsushi Hariki, Kwan-Woo Lee, and Jan Kuneš, *Antiferromagnetism in* $RuO_2$ *as d-wave Pomeranchuk instability*, Phys. Rev. B **99**, 184432 (2019).
[22] Lin-Ding Yuan, Zhi Wang, Jun-Wei Luo, Emmanuel I. Rashba, and Alex Zunger, *Giant momentum-dependent spin splitting in centrosymmetric low-z antiferromagnets*, Phys. Rev. B **102**, 014422 (2020).
[23] Ling Bai, Wanxiang Feng, Siyuan Liu, Libor Šmejkal, Yuriy Mokrousov, and Yugui Yao, *Altermagnetism: Exploring new frontiers in magnetism and spintronics*, Adv. Funct. Mater. **34**, 2409327 (2024).
[24] T. Jungwirth, J. Sinova, P. Wadley, D. Kriegner, H. Reichlová, F. Krizek, H. Ohno, and L. Šmejkal, *Altermagnetic spintronics*, Nat. Phys. (2026).
[25] Anna Birk Hellenes, Tomáš Jungwirth, Rodrigo Jaeschke-Ubiergo, Atasi Chakraborty, Jairo Sinova, and Libor Šmejkal, *P-wave magnets*, arXiv:2309.01607.
[26] Bjørnulf Brekke, Pavlo Sukhachov, Hans Gløckner Giil, Arne Brataas, and Jacob Linder, *Minimal models and transport properties of unconventional p-wave magnets*, Phys. Rev. Lett. **133**, 236703 (2024).
[27] Rinsuke Yamada *et al.*, *A metallic p-wave magnet with commensurate spin helix*, Nature (London) **646**, 837 (2025).
[28] Atasi Chakraborty, Anna Birk Hellenes, Rodrigo Jaeschke-Ubiergo, Tomás Jungwirth, Libor Šmejkal, and Jairo Sinova, *Highly efficient non-relativistic Edelstein effect in nodal p-wave magnets*, Nat. Commun. **16**, 7270 (2025).
[29] Zi-Ting Sun, Xilin Feng, Ying-Ming Xie, Benjamin T. Zhou, Jin-Xin Hu, and K. T. Law, *Pseudo-Ising superconductivity induced by p-wave magnetism*, Phys. Rev. B **112**, 214504 (2025).
[30] Qihang Liu, Xi Dai, and Stefan Blügel, *Different facets of unconventional magnetism*, Nat. Phys. **21**, 329 (2025).
[31] Jian-Keng Yuan, Zhiming Pan, and Congjun Wu, *Unconventional magnetism in spin-orbit coupled systems*, Phys. Rev. B **113**, 014426 (2026).
[32] Congjun Wu and Shou-Cheng Zhang, *Dynamic generation of spin-orbit coupling*, Phys. Rev. Lett. **93**, 036403 (2004).
[33] Congjun Wu, Kai Sun, Eduardo Fradkin, and Shou-Cheng Zhang, *Fermi liquid instabilities in the spin channel*, Phys. Rev. B **75**, 115103 (2007).
[34] Xun-Jiang Luo, Jin-Xin Hu, and K. T. Law, *Spin symmetry criteria for odd-parity magnets*, arXiv:2510.05512.
[35] Xiaobing Chen, Weizhao Chen, and Qihang Liu, *The rise of unconventional magnetism*, arXiv:2603.27505.
[36] Mengli Hu, Mikel I. Iraola, Paul McClarty, Jeroen van den Brink, and Maia G. Vergniory, *Non-collinear altermagnetic phases in the Mott insulator* $NiS_2$, arXiv:2603.01329.
[37] Zhenyu Xiao, Jianzhou Zhao, Yanqi Li, Ryuichi Shindou, and Zhi-Da Song, *Spin space groups: Full classification and applications*, Phys. Rev. X **14**, 031037 (2024).
[38] Yi Jiang, Ziyin Song, Tiannian Zhu, Zhong Fang, Hongming Weng, Zheng-Xin Liu, Jian Yang, and Chen Fang, *Enumeration of spin-space groups: Toward a complete description of symmetries of magnetic orders*, Phys. Rev. X **14**, 031039 (2024).
[39] Xiaobing Chen, Jun Ren, Yanzhou Zhu, Yutong Yu, Ao Zhang, Pengfei Liu, Jiayu Li, Yuntian Liu, Caiheng Li, and

Qihang Liu, *Enumeration and representation theory of spin space groups*, Phys. Rev. X **14**, 031038 (2024).

[40] Gemma de la Flor, Bernd Souvignier, Gotzon Madariaga, and Mois I. Aroyo, *Layer groups: Brillouin-zone and crystallographic databases on the Bilbao crystallographic server*, Acta Crystallogr. Sect. A **77**, 559 (2021).

[41] See Supplemental Material at http://link.aps.org/supplemental/10.1103/zy7s-j86r for details of minimal models, the mapping to altermagnetic phases, candidate materials, response-tensor analysis, and first-principles calculations, which includes Refs. [42–48].

[42] Yichi Zhang, Hua Bai, Jiankun Dai, Lei Han, Chong Chen, Shixuan Liang, Yanzhang Cao, Yingying Zhang, Qian Wang, Wenxuan Zhu, Feng Pan, and Cheng Song, *Electrical manipulation of spin splitting torque in altermagnetic* $RuO_2$, Nat. Commun. **16**, 5646 (2025).

[43] Yibo Fan, Qian Wang, and Wei Wang, *Robust magnetic-field-free perpendicular magnetization switching by manipulating spin polarization direction in* $RuO_2/[Pt/Co/Pt]$ *heterojunctions*, ACS Nano **18**, 26350 (2024).

[44] Y. Zhang, Y. Sun, H. Yang, J. Železný, Stuart P. P. Parkin, Claudia Felser, and Binghai Yan, *Strong anisotropic anomalous Hall effect and spin Hall effect in the chiral antiferromagnetic compounds* $mn_3x$ *(*$x = Ge$*, Sn, Ga, Ir, Rh, and Pt)*, Phys. Rev. B **95**, 075128 (2017).

[45] T. Farajollahpour, R. Ganesh, and K. V. Samokhin, *Berry curvature-induced transport signature for altermagnetic order*, npj Quantum Mater. **10**, 77 (2025).

[46] G. Kresse and J. Furthmüller, *Efficient iterative schemes for ab initio total-energy calculations using a plane-wave basis set*, Phys. Rev. B **54**, 11169 (1996).

[47] John P. Perdew, Kieron Burke, and Matthias Ernzerhof, *Generalized gradient approximation made simple*, Phys. Rev. Lett. **77**, 3865 (1996).

[48] Hendrik J. Monkhorst and James D. Pack, *Special points for Brillouin-zone integrations*, Phys. Rev. B **13**, 5188 (1976).

[49] Ran He, Dan Wang, Nannan Luo, Jiang Zeng, Ke-Qiu Chen, and Li-Ming Tang, *Nonrelativistic spin-momentum coupling in antiferromagnetic twisted bilayers*, Phys. Rev. Lett. **130**, 046401 (2023).

[50] Yunxi Qi, Jun Zhao, and Hui Zeng, *Spin-layer coupling in two-dimensional altermagnetic bilayers with tunable spin and valley splitting properties*, Phys. Rev. B **110**, 014442 (2024).

[51] Jianke Tian, Jia Li, Hengbo Liu, Yan Li, Ze Liu, Linyang Li, Jun Li, Guodong Liu, and Junjie Shi, *Spin-layer coupling in an altermagnetic multilayer: A design principle for spintronics*, Phys. Rev. B **111**, 035437 (2025).

[52] Samuel V. Gallego, J. Manuel Perez-Mato, Luis Elcoro, Emre S. Tasci, Robert M. Hanson, Koichi Momma, Mois I. Aroyo, and Gotzon Madariaga, *MAGNDATA: Towards a database of magnetic structures. I. The commensurate case*, J. Appl. Crystallogr. **49**, 1750 (2016).

[53] Marc Pernet, G. Quezel, Jean Coing-Boyat, and Félix Bertaut, *Structures magnétiques des chromates de cobalt et de nickel*, Bull. Minéral. **92**, 264 (1969).

[54] S. Kume, F. Kanamaru, Y. Shibasaki, M. Koizumi, K. Yasunami, and T. Fukuda, *Generation of high pressure oxygen and synthesis of* $CoCrO_4$ *with* $CrVO_4$ *type structure*, Rev. Sci. Instrum. **42**, 1856 (1971).

[55] Luis Elcoro, Jesus Etxebarria, J. Manuel Perez-Mato, and Emre S. Tasci, *Automatic calculation of symmetry-adapted tensors under spin-group symmetry: STENSOR, a new tool of the Bilbao crystallographic server*, J. Appl. Crystallogr. **59**, 640 (2026).

[56] H. A. Jahn, *Note on the Bhagavantam-Suryanarayana method of enumerating the physical constants of crystals*, Acta Crystallogr. **2**, 30 (1949).

[57] S. V. Gallego, J. Etxebarria, L. Elcoro, E. S. Tasci, and J. M. Perez-Mato, *Automatic calculation of symmetry-adapted tensors in magnetic and non-magnetic materials: A new tool of the Bilbao crystallographic server*, Acta Crystallogr. Sect. A **75**, 438 (2019).

[58] Jesus Etxebarria, J. Manuel Perez-Mato, Emre S. Tasci, and Luis Elcoro, *Crystal tensor properties of magnetic materials with and without spin–orbit coupling. Application of spin point groups as approximate symmetries*, Acta Crystallogr. Sect. A **81**, 317 (2025).

[59] Rui-Chun Xiao, Yuanjun Jin, Zhi-Fan Zhang, Zi-Hao Feng, Ding-Fu Shao, and Mingliang Tian, *TENSORSYMMETRY: A package to get symmetry-adapted tensors disentangling spin-orbit coupling effect and establishing analytical relationship with magnetic order*, Comput. Phys. Commun. **318**, 109872 (2026).

[60] Hikaru Watanabe, Kohei Shinohara, Takuya Nomoto, Atsushi Togo, and Ryotaro Arita, *Symmetry analysis with spin crystallographic groups: Disentangling effects free of spin-orbit coupling in emergent electromagnetism*, Phys. Rev. B **109**, 094438 (2024).

[61] Rafael González-Hernández, Libor Šmejkal, Karel Výborný, Yuta Yahagi, Jairo Sinova, Tomá š Jungwirth, and Jakub Železný, *Efficient electrical spin splitter based on nonrelativistic collinear antiferromagnetism*, Phys. Rev. Lett. **126**, 127701 (2021).

[62] Jakub Železný, Yang Zhang, Claudia Felser, and Binghai Yan, *Spin-polarized current in noncollinear antiferromagnets*, Phys. Rev. Lett. **119**, 187204 (2017).

[63] Mengli Hu, Oleg Janson, Claudia Felser, Paul McClarty, Jeroen van den Brink, and Maia G. Vergniory, *Spin Hall and Edelstein effects in chiral non-collinear altermagnets*, Nat. Commun. **16**, 8529 (2025).

[64] Ziyin Song, *SSGClassify*, GitHub repository, https://github.com/zine-phy/SSGClassify (2026).